



1 Chemical composition, structures, and light absorption of N-containing
2 aromatic compounds emitted from burning wood and charcoal in
3 household cookstoves

4

5 Mingjie Xie¹, Zhenzhen Zhao¹, Amara L. Holder², Michael D. Hays², Xi Chen², Guofeng Shen³,
6 James J. Jetter², Qin'geng Wang⁴

7

8 ¹Collaborative Innovation Center of Atmospheric Environment and Equipment Technology,
9 Jiangsu Key Laboratory of Atmospheric Environment Monitoring and Pollution Control, School
10 of Environmental Science and Engineering, Nanjing University of Information Science &
11 Technology, 219 Ningliu Road, Nanjing 210044, China

12 ²Center for Environmental Measurement and Modeling, Office of Research and Development, U.S.
13 Environmental Protection Agency, 109 T.W. Alexander Drive, Research Triangle Park, NC 27711,
14 USA

15 ³Laboratory for Earth Surface Processes, College of Urban and Environmental Sciences, Peking
16 University, Beijing 100871, China

17 ⁴State Key Laboratory of Pollution Control and Resource Reuse, Nanjing University, Nanjing
18 210023, China

19

20 *Correspondence to:* Mingjie Xie (mingjie.xie@colorado.edu; mingjie.xie@nuist.edu.cn)

21

22 Tel: +1-18851903788;

23 Fax: +86-25-58731051;

24 Mailing address: 219 Ningliu Road, Nanjing, Jiangsu, 210044, China

25



26 **Abstract**

27 N-containing aromatic compounds (NACs) are an important group of light-absorbing
28 molecules in the atmosphere. They are often observed in combustion emissions, but their chemical
29 formulas and structural characteristics remain uncertain. In this study, red oak wood and charcoal
30 fuels were burned in cookstoves using the standard water boiling test (WBT) procedure.
31 Submicron aerosol particles in the cookstove emissions were collected using quartz (Q_f) and
32 polytetrafluoroethylene (PTFE) filter membranes positioned in parallel. A back-up quartz filter
33 (Q_b) was also installed downstream of the PTFE filter to evaluate the effect of sampling artifact on
34 NACs measurements. Liquid chromatography-mass spectroscopy (LC-MS) techniques identified
35 seventeen NAC chemical formulas in the cookstove emissions. The average concentrations of total
36 NACs in Q_b samples ($0.37 \pm 0.31 - 1.78 \pm 0.78 \mu\text{g m}^{-3}$) were greater than 50% of those observed
37 in the Q_f samples ($0.47 \pm 0.40 - 3.54 \pm 1.63 \mu\text{g m}^{-3}$), and the Q_b to Q_f mass ratios of individual
38 NACs had a range of 0.02 – 2.71, indicating that the identified NACs might have substantial
39 fractions remaining in the gas-phase. In comparison to other sources, cookstove emissions from
40 red oak or charcoal fuels did not exhibit unique NAC structural features, but had distinct NACs
41 composition. However, before identifying NACs sources by combining their structural and
42 compositional information, the gas-particle partitioning behaviors of NACs should be further
43 investigated. The average contributions of total NACs to the light absorption of organic matter at
44 $\lambda = 365 \text{ nm}$ ($1.10 - 2.58\%$) in Q_f samples are much lower than those in Q_b samples ($10.7 - 21.0\%$).
45 These results suggest that more research is needed to understand the chemical and optical
46 properties of gaseous chromophores and heavier molecular weight (e.g., $\text{MW} > 500 \text{ Da}$) entities
47 in particulate matter.

48

49



50 **1 Introduction**

51 In the developing world, 2.8 billion people burn solid fuels in household cookstoves for
52 domestic activities such as heating and cooking (Bonjour et al., 2013). A variety of gaseous and
53 particulate phase pollutants — carbon monoxide (CO), nitrogen oxides (NO_x), volatile organic
54 compounds (VOCs), fine particulate matter with aerodynamic diameter $\leq 2.5 \mu\text{m}$ (PM_{2.5}), black
55 carbon (BC), organic carbon (OC), etc. — are emitted from cookstoves largely due to incomplete
56 combustion (Jetter et al., 2012; Shen et al., 2012; Wathore et al., 2017). In China, the relative
57 contributions of residential coal and biomass burning (BB) to annual PM_{2.5} emissions decreased
58 from 47% (4.32 Tg) in 1990 to 34% (4.39 Tg) in 2005 due to the growth in industrial emissions
59 (Lei et al., 2011). Although, more than half of BC (> 50 %) and OC (> 60 %) emissions are
60 attributed to residential coal and BB in both China and India (Cao et al., 2006; Klimont et al., 2009;
61 Lei et al., 2011).

62 Household solid fuel combustion is a leading human health risk, especially for women and
63 children who tend to spend more time indoors than men (Anenberg et al., 2013). Estimates show
64 that exposures to PM_{2.5} from domestic solid fuel combustion caused 3.9 million premature deaths
65 and ~4.8% of lost healthy life years (Smith et al., 2014). In addition, the emissions of carbonaceous
66 aerosols from cookstoves can affect the Earth's radiative balance by absorbing and scattering
67 incoming solar radiation (Lacey and Henze, 2015; Aunan et al., 2009). BC is the most efficient
68 light absorber in the atmosphere, while the total aerosol absorption, including that from OC, is still
69 highly uncertain (Yang et al., 2009; Park et al., 2010; Feng et al., 2013; Wang et al., 2014; Tuccella
70 et al., 2020). Multiple field and laboratory studies have demonstrated that OC in both primary PM
71 emissions (e.g., biomass and fossil fuel combustions) and secondary organic aerosol (SOA) feature
72 a range of absorptivity in the near ultraviolet (UV) and short visible wavelength regions



73 (Nakayama et al., 2010; Forrister et al., 2015; Lin et al., 2015; De Haan et al., 2017; Xie et al.,
74 2017a, b, 2018). The light absorbing OC fraction is often referred to as “brown carbon” (BrC).
75 Unlike open BB (e.g., forest, grassland, and cropland fires) — one of the most important primary
76 sources for organic aerosols (Bond et al., 2004) — the light absorption of BrC from household
77 cookstove emissions is rarely investigated. Sun et al. (2017) found that the BrC absorption from
78 residential coal burning accounted for 26.5% of the total aerosol absorption at 350~850 nm. BrC
79 from wood combustion in cookstoves has a greater mass specific absorption than that from open
80 BB over the wavelength range of 300 – 550 nm (Xie et al., 2018). These results suggest that
81 cookstove emissions may also be an important BrC source, which needs to be accounted for
82 separately from open BB.

83 Organic molecular markers (OMMs) are commonly used in receptor-based source
84 apportionment of carbonaceous aerosols (Jaeckels et al., 2007; Shrivastava et al., 2007; Xie et al.,
85 2012). Polycyclic aromatic hydrocarbons (PAHs) and their derivatives are a group of OMMs with
86 light absorption properties dependent on ring number or the degree of conjugation (Samburova et
87 al., 2016). As discussed in Xie et al. (2019), PAHs are generated from a multitude of combustion
88 processes (e.g., BB, fossil fuel combustion) (Chen et al., 2005; Riddle et al., 2007; Samburova et
89 al., 2016), and their ubiquitous nature makes them less than ideal OMMs for BrC source attribution.
90 Because of the specific toxicological concern raised by PAHs — they are mutagenic and
91 carcinogenic [International Agency for Research on Cancer (IARC), 2010] — source emission
92 factors, ambient levels, and potential health effects of PAHs are investigated exhaustively
93 (Ravindra et al., 2008; Kim et al., 2013). Similar to PAHs, N-containing aromatic compounds
94 (NACs) are a group of BrC chromophores commonly detected in ambient PM and source
95 emissions. Zhang et al. (2013) and Teich et al. (2017) calculated the absorption of individual NACs



96 in aqueous extracts of ambient PM, the total of which explained ~3% of the bulk extract absorption
97 at 365 – 370 nm. With the same approach, Xie et al. (2017a, 2019) found that the absorbance due
98 to NACs in BB or secondary OC was 3 – 10 times higher than their mass contributions. Lin et al.
99 (2016, 2017) estimated an absorbance contribution of 50 – 80% from NACs in BB OC directly
100 from their high-performance liquid chromatography (HPLC)/photodiode array (PDA) signals,
101 which are subject to considerable uncertainty due to the co-elution of other BrC chromophores,
102 (e.g., PAHs and their derivatives). These results indicate that NACs are strong BrC chromophores,
103 but the estimation of their contributions to BrC absorption depends largely on how well they are
104 chemically characterized. Nitrophenols, methyl nitrophenols, nitrocatechols and methyl
105 nitrocatechols (including isomers) are typical atmospheric NACs (Claeys et al., 2012; Desyaterik
106 et al., 2013; Zhang et al., 2013). These NACs can be generated from BB (Lin et al., 2016, 2017;
107 Xie et al., 2019), fossil fuel combustion (Lu et al., 2019), and the reactions of aromatic volatile
108 organic compounds (VOCs) with reactive nitrogen species (e.g., NO_x) (Xie et al., 2017a), and are
109 not unique to specific sources (e.g., BB). By using a HPLC interfaced to a diode array detector
110 (DAD) and quadrupole (Q) time-of-flight mass spectrometer (ToF-MS), Xie et al. (2019) found
111 that BB NACs contain methoxy and cyanate groups. Nitronaphthol, nitrobenzenetriol, and methyl
112 nitrobenzenetriol are characteristic NACs for NO_x-based chamber reactions of naphthalene,
113 benzene, and *m*-cresol, respectively (Xie et al., 2017a). Yet, few studies have investigated the
114 composition of NACs from household cookstove emissions (Fleming et al., 2018; Lu et al., 2019).

115 The present study aims to characterize NACs in PM_{2.5} from burning red oak and charcoal in
116 a variety of cookstoves and calculate their contributions to bulk OC absorption. The absorption of
117 OC in solvent extracts of cookstove emissions were measured in our previous work (Xie et al.,
118 2018). Presently, NACs are identified and quantified using an earlier described HPLC/DAD-Q-



119 ToF-MS system. In addition, the NACs adsorbed on a backup quartz filter downstream of a
120 polytetrafluoroethylene (PTFE) membrane filter are analyzed, to evaluate the potential for
121 sampling artifacts of NACs in $PM_{2.5}$. This work unveils BrC composition at a molecular level and
122 increases the understanding of BrC chromophores and their sources. It also shows that further
123 identification of large molecules (e.g., > 500 Da) may better explain BrC absorption in the particle
124 phase and that understanding the light absorption of gaseous chromophores is important for the
125 future.

126 **2 Methods**

127 ***2.1. Cookstove emissions sampling***

128 Details of the cookstove emission test facility, fuel-cookstove combinations, water boiling
129 test (WBT) protocol, and $PM_{2.5}$ emissions sampling were described previously in Jetter et al. (2012)
130 and Xie et al. (2018). Briefly, the cookstove emissions tests were performed at the U.S. EPA
131 cookstove test facility in Research Triangle Park, NC. Three fuels (red oak wood, lump charcoal,
132 and 1-K kerosene) were burned in fuel-specific cookstoves. Due to the limited sample number (n
133 = 6) and low OC emissions from kerosene burning, only red oak and charcoal burning samples
134 were used for NACs analysis. Low moisture (~10%) oak and charcoal fuels were burned with five
135 specific-designed cookstove types (Tables S1 and S2); high moisture (~30%) oak fuels were
136 burned in one cookstove (Jiko Poa). Emissions tests for each fuel-cookstove combination were
137 performed in triplicate. The WBT protocol (version 4) (Global Alliance for Clean Cookstoves,
138 2014) is designed to measure cookstove power, energy efficiency and fuel use and utilizes cold-
139 start (CS) high power, hot-start (HS) high power, and simmer (SIM) low power phases. Gaseous
140 pollutant (e.g., CO, methane (CH_4)) emissions were monitored continuously, and $PM_{2.5}$ filter
141 samples were collected during each test phase of the WBT protocol. A quartz-fiber filter (Q_f) and



142 a PTFE membrane filter positioned in parallel collected PM_{2.5} isokinetically at a flow rate of 16.7
143 L min⁻¹. Adsorption artifact was evaluated using a quartz-fiber back-up filter (Q_b) installed
144 downstream of the PTFE filter during PM_{2.5} sampling.

145 **2.2. Chemical analysis**

146 The OC and elemental carbon (EC) emissions and UV-Vis light absorption properties (BrC)
147 of methanol-extracted cookstove particles were reported in Xie et al. (2018). Details of the method,
148 sample selection, and measurement results are summarized in supplementary information (Text
149 S1, Tables S1 and S2). The Q_f and Q_b sample extraction and subsequent analysis for NACs were
150 conducted as described in Xie et al. (2019). In brief, an aliquot of each filter sample was pre-spiked
151 with 250 ng nitrophenol-d4 (internal standard) and extracted ultrasonically twice for 15 min in 3-
152 5 mL of methanol. After filtration (30 mm diameter, ×0.2 μm pore size, PTFE filter), the extract
153 volume was reduced to ~500 μL with rotary evaporation prior to HPLC/DAD-MS (Q-ToF)
154 analysis. The NACs targeted in this work were chromatographed using an Agilent 1200 Series
155 HPLC equipped with a Zorbax Eclipse Plus C18 column (2.1 mm × 100 mm, 1.8 μm particle size;
156 Agilent Technologies). The gradient separation was performed using water (eluent A) and
157 methanol (eluent B) containing 0.2% acetic acid (v/v) with a total flow rate of 0.2 mL min⁻¹. The
158 eluent B fraction was held at 25% for 3 min, increased to 100% over the next 7 min, where it was
159 held for 22 min, and then returned to 25% over 5 min. An Agilent 6520 Q-ToF MS equipped with
160 a multimode ion source operating in electrospray ionization (ESI) negative (-) mode was used to
161 determine the chemical formula, molecular weight (MW), and quantity of each target compound.
162 All sample extracts were analyzed in full scan mode over 40–1000 Da. A mass accuracy of ± 10
163 ppm was selected for compound identification and quantification. Samples with individual NACs
164 exhibiting the highest MS signal intensities in full scan mode were re-examined in targeted MS-



165 MS mode using a collision-induced dissociation (CID) technique. The MS-MS spectra of target
166 NACs $[M-H]^-$ ions were acquired to deduce structural information. Similar to bulk carbon and
167 light absorption measurements, NACs were primarily determined for CS- and HS-phase samples
168 with substantial OC loadings.

169 Due to the limited availability of authentic standards, many of the NACs identified in
170 cookstove combustion samples were quantified using surrogate compounds with similar MW or
171 structures. An internal standard method with a 9-point calibration curve ($\sim 0.01 - 2 \text{ ng } \mu\text{L}$) was
172 applied for quantification of concentrations. The compounds represented by each identified NAC
173 formula were quantified individually and combined to calculate the mass ratio of total NACs to
174 OC ($\mu\text{g m}^{-3}$) $\times 100\%$ ($\text{tNAC}_{\text{OC}}\%$). Presently, the organic matter (OM) to OC ratio was not
175 measured or estimated for cookstove combustion emissions, so $\text{tNAC}_{\text{OC}}\%$ could be up to 2 times
176 greater than the contributions of NACs to OM (Reff et al., 2009; Turpin and Lim, 2001). Table S3
177 lists the chemical formulas, proposed structures, and standard assignments for the NACs identified
178 here. The quality assurance and control (QA/QC) procedures for filter extraction and instrumental
179 analysis were the same as Xie et al. (2017a, 2019). NACs were not detected in field blank and
180 background samples. The average recoveries of NAC standards on pre-spiked blank filters ranged
181 from 75.1% to 116%, and the method detection limit had a range of 0.70–17.6 pg.

182 **2.3. Data analysis**

183 In Xie et al. (2017a), the DAD measurement directly identified the chemical compounds in
184 chamber SOA responsible for light absorption in the near UV and visible light ranges. However,
185 no light absorption from individual NACs was detected in the DAD chromatograms from open BB
186 (Xie et al., 2019) and cookstove emissions (this work). So the contributions of individual NACs



187 to light absorption coefficient (Abs_{λ} , Mm^{-1}) for each sample extract at 365 nm ($Abs_{365,iNAC}\%$) were
188 calculated using the method described in Xie et al. (2017a, 2019):

$$189 \quad Abs_{365,iNAC}\% = \frac{C_{iNAC} \times MAC_{365,iNAC}}{Abs_{365}} \times 100\% \quad (1)$$

190 where C_{iNAC} is the mass concentration ($ng\ m^{-3}$) of individual NACs, and $MAC_{365,iNAC}$ is the mass
191 absorption coefficient (MAC_{λ} , $m^2\ g^{-1}$) of individual NACs at 365 nm. Abs_{365} is the light absorption
192 coefficient (Mm^{-1}) of each sample extract at 365 nm, and has been widely used to represent BrC
193 absorption (Chen and Bond, 2010; Hecobian et al., 2010; Liu et al., 2013). Each NAC compound
194 was assumed to absorb as a standard (Table S3), of which the $MAC_{365,iNAC}$ value was obtained
195 from Xie et al. (2017a, 2019) and listed in Table S4. In this work, Student's t -test was used to
196 determine if the means of two sets of data are significantly different from each other, and a p value
197 less than 0.05 indicates significant difference.

198 **3 Results and discussion**

199 ***3.1 Summary of total NACs concentration from cookstove emissions***

200 Table 1 summarizes the average concentrations of total NACs and average $tNAC_{OC}\%$ for
201 Q_f and Q_b by fuel type and WBT phase. Filter samples of emissions from burning red oak wood
202 show significantly ($p < 0.05$) higher average total NAC concentrations and $tNAC_{OC}\%$ than the
203 charcoal burning samples. Wood burning generates more volatile aromatic compounds (e.g.,
204 phenols, PAHs) than charcoal burning (Kim Oanh, et al., 1999), and NACs can form when
205 aromatic compounds and reactive nitrogen (e.g., NO_x) are present during solid fuel combustion
206 (Lin et al., 2016, 2017). While burning red oak, emissions from the CS and HS phases show similar
207 average NAC concentrations and $tNAC_{OC}\%$ (Table 1). Additionally, burning low or high moisture
208 red oak in the Jiko Poa stove shows no significant ($p > 0.05$) difference in $tNAC_{OC}\%$ (Tables S5
209 and S6). Thus, the NAC and OC emissions from red oak burning are less likely influenced by



210 WBT phase or fuel moisture. For charcoal fuel samples, compared with the CS-phase, the HS-
211 phase shows significantly higher ($p < 0.05$) average NAC concentrations. This is likely due to the
212 increase in OC with the HS phase (Table 1), as the average $tNAC_{OC}\%$ values are much closer for
213 the CS- ($0.38 \pm 0.25\%$) and HS-phases ($0.31 \pm 0.22\%$).

214 Several studies have placed a quartz-fiber filter behind a PTFE filter to evaluate the positive
215 adsorption artifact — adsorption of gas-phase compounds onto particle filter media, “blow-on”
216 effect (Peters et al., 2000; Subramanian et al., 2004; Watson et al., 2009; Xie et al., 2014). This
217 method is expected to provide a consistent estimate irrespective of sampling time, but may over
218 correct the positive artifact by 16–20% due to volatilization of OC off the upstream PTFE filter
219 (negative artifact, “blow-off” effect) (Subramannian et al., 2004). The present study is the first to
220 consider sampling artifact when measuring semivolatile NACs. This concept merits consideration
221 as quantification of particle-phase NACs may be subject to large uncertainty. Table 1 shows that
222 the average concentrations of total NACs on Q_b ($0.37 \pm 0.31 - 1.78 \pm 0.78 \mu\text{g m}^{-3}$) are greater than
223 50% and 70% of those on Q_f ($0.47 \pm 0.40 - 3.54 \pm 1.63 \mu\text{g m}^{-3}$) for red oak and charcoal burning,
224 respectively. The average Q_b to Q_f ratio in percentage using OC concentrations is 2-3 times lower
225 ($14.8 \pm 3.87 - 38.8 \pm 18.9\%$). Hence, the NACs identified in this work are present in the relatively
226 volatile bulk OC fraction emitted from cookstoves, and the NACs in the Q_f samples may also be
227 present in the gas-phase in the atmosphere. Charcoal burning emissions show even higher ($p < 0.05$)
228 Q_b to Q_f total NAC mass ratios (CS $87.7 \pm 34.2\%$, HS $143 \pm 51.4\%$) than red oak burning (CS 53.0
229 $\pm 10.6\%$, HS $55.1 \pm 24.7\%$), which is largely due to the higher OC loads on Q_f samples from red
230 oak burning. Xie et al. (2018) assumed previously that the Q_b -adsorbed OC represented the
231 positive sampling artifact only, and adjusted the light absorbing properties of OC on Q_f by
232 subtracting Abs_{365} and OC of Q_b samples directly. In this study, the high Q_b to Q_f ratios of total



233 NACs indicate that the volatilization of NACs from upstream PTFE filter cannot be neglected, but
234 the relative contributions of positive and negative artifacts to Q_b measurements are unknown.
235 Therefore, the measurement results of NACs in Q_f and Q_b samples were provided separately, and
236 no correction was conducted for Q_f measurements in this work. Since the gaseous NACs adsorbed
237 on Q_b samples depends on Q_f loadings, $tNAC_{OC}\%$ and total NACs concentrations in each Q_f - Q_b
238 pair from matching tests are significantly correlated ($p < 0.05$, Fig. S1a, b, d, and e).

239 Along with modified combustion efficiency (MCE), the EC/OC and BC/OA (organic
240 aerosol) ratios were used previously as indicators of biomass burning conditions (McMeeking et
241 al., 2014; Pokhrel et al., 2016). Here the burn condition indicates general flame intensity or
242 combustion temperature (Chen and Bond, 2010; Saleh et al., 2014), and is parameterized to
243 investigate combustion processes (e.g., pyrolysis). The MCE, EC/OC and BC/OA ratios are key
244 to understanding particulate OC absorptivity (Saleh et al., 2014; Lu et al., 2015) and NACs
245 formation from open BB (Xie et al., 2019). Presently, the relationships of $tNAC_{OC}\%$ versus EC/OC
246 for Q_f samples are shown in Fig. S1c and f by fuel type. Because no significant difference was
247 observed for average total NACs concentrations, $tNAC_{OC}\%$, and EC/OC ratios when testing CS-
248 versus HS- phases during red oak fuel burning, the CS- and HS-phases were pooled for a regression
249 analysis. The $tNAC_{OC}\%$ of Q_f samples positively correlate ($r = 0.83$, $p < 0.05$) with EC/OC for red
250 oak burning (Fig. S1c), as observed in Xie et al. (2019) for open BB, which suggests that burn
251 conditions influence NACs formation during BB. Note that the NAC concentrations on Q_f were
252 possibly adsorbed while in a gaseous state, while EC is particle phase.

253 Like MAC_{365} and \dot{A}_{abs} in Q_f samples for charcoal burning (Xie et al., 2018), $tNAC_{OC}\%$
254 derived from the same samples did not correlate with EC/OC ratios in this work (Fig. S1f). Xie et
255 al. (2018) found that the HS-phase for charcoal burning had average OC EFs 5–10 times higher



256 than the CS-phase, while the EC EFs decreased by more than 90% from the CS- to HS-phase, so
257 the EC/OC for charcoal burning is sensitive to the initial temperature in the cookstove, and cannot
258 be used to predict burn conditions, BrC absorption, or NACs formation.

259 *3.2 Composition of NACs in Q_f and Q_b*

260 During solid fuel combustion, NACs may form from aromatic compounds (e.g., substituted
261 phenols) and reactive nitrogen species (e.g., NH_3 , NO_x , and HONO) in both the gas- and particle-
262 phase (Harrison et al., 2005; Kwamena and Abbatt, 2008; Lu et al., 2011; Lin et al., 2016, 2017).
263 Aromatic hydrocarbons are produced during fuel pyrolysis (Simoneit et al., 1993; Simoneit, 2002;
264 Kaal et al., 2009). Oxidation of fuel derived nitrogen, rather than molecular nitrogen in air, is the
265 major formation pathway of reactive nitrogen species (Glarborg et al., 2003).

266 Presently, seventeen chemical formulas were identified as NACs in cookstove emissions,
267 several of which are widely observed in ambient air and open BB particles (e.g., $\text{C}_6\text{H}_5\text{NO}_3$,
268 $\text{C}_6\text{H}_5\text{NO}_4$) (Claeys et al., 2012; Zhang et al., 2013; Lin et al., 2016, 2017; Xie et al., 2019). Figure
269 1 shows the average concentrations (ng m^{-3}) of individual NACs in Q_f and Q_b samples by fuel type
270 and WBT phase. The corresponding average mass ratios of individual NACs to OC $\times 100\%$
271 ($\text{iNAC}_{\text{OC}}\%$) are shown in Fig. S2. Details of the NACs composition expressed in $\text{iNAC}_{\text{OC}}\%$ for
272 each fuel-cookstove experiment are given in Tables S5–S8.

273 Generally, the CS and HS phases have consistent NAC profiles for red oak combustion
274 (Figs. 1a, b and S2a, b). $\text{C}_{10}\text{H}_7\text{NO}_3$ has the highest average concentrations (CS- Q_f 1003 ± 803 ng
275 m^{-3} , HS- Q_f 1149 ± 1053 ng m^{-3}) and $\text{iNAC}_{\text{OC}}\%$ (CS- Q_f $0.45 \pm 0.80\%$, HS- Q_f $0.43 \pm 0.79\%$) on Q_f ,
276 followed by $\text{C}_{11}\text{H}_9\text{NO}_3$, $\text{C}_{10}\text{H}_{11}\text{NO}_5$, and $\text{C}_{11}\text{H}_{13}\text{NO}_5$. Q_b samples of red oak combustion emissions
277 have similar NACs profiles and characteristic species (e.g., $\text{C}_{10}\text{H}_7\text{NO}_3$, $\text{C}_{11}\text{H}_9\text{NO}_3$) as Q_f samples,
278 and the individual NAC distributions in Q_b to Q_f samples are similar between the CS- and HS-



279 phases (Fig. 1a, b). It appears that the formation of NACs from red oak burning in cookstoves
280 depends largely on burn conditions reflected by EC/OC ratios (Fig. S1c) rather than WBT phases.
281 Among the 17 identified NACs from red oak burning, $C_8H_5NO_2$ and $C_{11}H_{13}NO_6$ have the lowest
282 Q_b to Q_f ratios (2.42 – 12.6%, Fig. 1a, b), indicating their low volatility. The low volatility of
283 $C_{11}H_{13}NO_6$ might be due to its relatively high MW; while $C_8H_5NO_2$ has the second lowest MW
284 and its structure likely contains functional groups that decrease vapor pressure (e.g., carboxyl
285 group) (Donahue et al., 2011).

286 Charcoal burning generated high abundances of $C_8H_9NO_5$, $C_{11}H_9NO_3$, and $C_{10}H_7NO_3$ for
287 both CS ($86.6 \pm 98.7 - 170 \pm 200 \text{ ng m}^{-3}$) and HS ($97.1 \pm 38.5 - 178 \pm 104 \text{ ng m}^{-3}$) phases (Figs.
288 1c, d and S2c, d). Average concentrations of $C_8H_9NO_5$, $C_{11}H_9NO_3$, and $C_{10}H_7NO_3$ in the Q_b (62.0
289 $\pm 64.9 - 198 \pm 115 \text{ ng m}^{-3}$) and Q_f samples were comparable. However, the iNAC_{OC}% of these
290 compounds are $1.45 \pm 0.68 - 5.16 \pm 2.84$ times higher in Q_b (iNAC_{OC}%, $0.11 \pm 0.18 - 0.46 \pm$
291 0.69%) than in Q_f samples ($0.052 \pm 0.067 - 0.14 \pm 0.15\%$). High levels of $C_6H_5NO_4$, $C_7H_7NO_4$,
292 and $C_8H_9NO_4$ were also observed in the HS phase for charcoal burning (Fig. 1d). These compounds
293 in Q_b samples had average concentrations ($222 \pm 132 - 297 \pm 277 \text{ ng m}^{-3}$) 22.6 – 80.8% higher
294 than in Q_f samples ($150 \pm 118 - 181 \pm 111 \text{ ng m}^{-3}$). As such, the charcoal HS phase generates more
295 low MW NACs (e.g., $C_6H_5NO_4$, $C_7H_7NO_4$) than the CS phase, and the initial temperature in the
296 cookstove has an impact on NAC formation from charcoal burning.

297 As mentioned in section 3.1, using a Q_b has been widely applied to evaluate the positive
298 sampling artifact for OC and semivolatile organic compounds. This method might only work for
299 bulk PM, OC, and low volatile organic compounds, of which the concentrations in Q_b samples are
300 much lower than Q_f samples and usually presumed to be due to positive adsorption artifacts only
301 (Subramanian et al., 2004; Watson et al., 2009). In this work, the average Q_b to Q_f mass ratios of



302 the 17 individual NACs ranged from $54.3 \pm 24.5\%$ to $135 \pm 52.4\%$, and the evaporation of NACs
303 from Q_f (negative artifact) is unknown. As a result, the particle-phase NAC concentrations cannot
304 be calculated by simply subtracting Q_b measurements from those of Q_f . Considering that most of
305 the Q_f and Q_b samples were collected near ambient temperature (Table S2, ~ 25 °C), some of the
306 identified NACs (e.g., 4-nitrophenol) may have substantial gas-phase concentrations (Li et al.,
307 2020), and the composition of NACs derived from Q_f measurements alone can be biased due to
308 the lack of gas-phase measurements. Future work is needed to evaluate the composition of NACs
309 from emission sources in both the particle and gas phases.

310 **3.3 Identification of NACs structures**

311 Figures S3 and S4 exhibited extracted ion chromatograms (EICs) and MS-MS spectra of
312 the 17 identified NACs. For comparison, the MS-MS spectra of standard compounds used in this
313 work are obtained from Xie et al. (2017a, 2019) and shown in Fig. S5. Among all identified NAC
314 formulas, $C_{10}H_7NO_3$ was detected in each fuel-cookstove experiment (Tables S5 – S8) and showed
315 the highest concentrations in emissions from burning red oak (Fig. 1a, b). The MS-MS spectrum
316 of $C_{10}H_7NO_3$ (Fig. S4l) is like 2-nitro-1-phenol (Fig. S5g) but shows a ~ 1 min difference in
317 retention time (Fig. S3i 10.9 min, 2-nitro-1-phenol 11.8 min). $C_{10}H_7NO_3$ is presumed to be an
318 isomer of 2-nitro-1-phenol with a nitronaphthol structure. $C_{11}H_9NO_3$ has a degree of unsaturation
319 and a fragmentation pattern (Fig. S4q) like $C_{10}H_7NO_3$ and is likely a structural isomer of methyl
320 nitronaphthol. $C_6H_5NO_3$, $C_7H_7NO_3$, $C_6H_5NO_4$, and $C_7H_7NO_4$ are commonly detected in
321 combustion emissions (Lin et al., 2016, 2017; Xie et al., 2017a) and atmospheric particles (Claeys
322 et al., 2012; Zhang et al., 2013). $C_6H_5NO_3$ and $C_6H_5NO_4$ are identified as 4-nitrophenol and 4-
323 nitrocatechol using authentic standards (Figs. S4a, d and S5a, c). $C_7H_7NO_3$ has two isomers (Fig.
324 S3b) and the compound eluting at 9.98 min has the same retention time and MS-MS spectrum (Fig.



325 S4c) as 2-methyl-4-nitrophenol (Fig. S5b). In ambient PM and chamber SOA, $C_7H_7NO_4$ was
326 identified using standard compounds as a series of methyl-nitrocatechol isomers (4-methyl-5-
327 nitrocatechol, 3-methyl-5-nitrocatechol, and 3-methyl-6-nitrocatechol) (Iinuma et al., 2010).
328 According to the HPLC-Q-ToFMS data for $C_7H_7NO_4$ identified in Iinuma et al. (2010) and our
329 previous studies (Xie et al., 2017a, 2019), the two $C_7H_7NO_4$ isomers in Fig. S3d are likely 4-
330 methyl-5-nitrocatechol and 3-methyl-6-nitrocatechol, respectively. Here we cannot rule out the
331 presence of 3-methyl-5-nitrocatechol, which may co-elute with 4-methyl-5-nitrocatechol (Iinuma
332 et al., 2010). In Fig. S4k, o, and p, the MS-MS spectra of $C_7H_7NO_5$, $C_8H_7NO_5$, and $C_8H_9NO_5$ all
333 show a loss of $CH_3 + NO$ (or NO_2) + CO. The loss of CH_3 is typically due to a methoxy group in
334 NAC molecules, and NO (or NO_2) and CO loss is commonly observed for NACs with more than
335 one phenoxy group (Xie et al., 2019). So methoxy nitrophenol is the proposed skeleton for
336 $C_7H_7NO_5$, $C_8H_7NO_5$, and $C_8H_9NO_5$. Other functional groups were estimated using their chemical
337 formulas and degree of unsaturation as a basis (Table S3).

338 The present study quantifies $C_8H_7NO_4$ and $C_9H_9NO_4$ using 2-methyl-5-benzoic acid
339 ($C_8H_7NO_4$) and 2,5-dimethyl-4-nitrobenzoic acid ($C_9H_9NO_4$), respectively. The fragmentation
340 patterns of $C_8H_7NO_4$ (Fig. S4g, h) and $C_9H_9NO_4$ compounds (Fig. S4m, n) are different from their
341 corresponding surrogates (Fig. S5f, h) and loss of CO_2 is not observed, so $C_8H_7NO_4$ and $C_9H_9NO_4$
342 compound structures do not include a carboxyl group. The MS-MS spectra of $C_8H_7NO_4$ eluting at
343 8.14 min (Fig. S3e) and $C_9H_9NO_4$ eluting at 9.22 min (Fig. S3j) indicate the loss of OCN (Fig.
344 S4g, m), suggesting benzoxazole/benzisoxazole structure or the presence of cyanate ($-O-C\equiv N$) or
345 isocyanate ($-O=C=N$) groups. Mass spectra of selected standard compounds (Fig. S5i-n) in our
346 previous work (Xie et al. 2019) show the loss of an OCN group only happens during the
347 fragmentation of phenyl cyanate. Thus, the $C_8H_7NO_4$ and $C_9H_9NO_4$ isomers containing OCN



348 indicate a phenyl cyanate feature. However, the fragmentation mechanism related to the loss of a
349 single nitrogen for the second $C_8H_7NO_4$ isomer (Fig. S3e, Fig. S4h) is unknown and requires
350 further study. The MS-MS spectrum of the second $C_9H_9NO_4$ isomer had dominant ions at m/z 194
351 ($[M-H]^-$), 164 (loss of NO), and 149 (loss of NO + CH_3). Compared with the MS-MS spectra of
352 4-nitrophenol and 2-methyl-4-nitrophenol (Fig. S5a, b), the second $C_9H_9NO_4$ isomer is likely a
353 methoxy nitrophenol with an extra ethyl group.

354 The EIC signal of $C_8H_9NO_4$ in Fig. S3f comprises at least 3-4 isomers, and the MS-MS
355 spectra are always dominated by ions at m/z 182 ($[M-H]^-$), 152 (loss of NO), and 137 (loss of NO
356 + CH_3) with some changes in relative abundance. The fragmentation mechanism of $C_8H_9NO_4$
357 represented by the MS-MS spectrum in Fig. S4i is consistent with that of the second $C_9H_9NO_4$
358 isomer (Fig. S4n), so the $C_8H_9NO_4$ might also have a methoxy nitrophenol skeleton.

359 Unlike other NACs, $C_8H_5NO_2$ was only detected in samples from red oak burning in the
360 Jiko Poa and charcoal burning in the Éclair (Tables S5 – S8). The average mass ratios of $C_8H_5NO_2$
361 in Q_b to Q_f samples for red oak burning are less than 15% (CS phase 2.42%, HS phase 12.6%),
362 and $C_8H_5NO_2$ was not detected in any Q_b samples for charcoal burning. The MS-MS spectrum of
363 $C_8H_5NO_2$ is characterized by CO_2 loss (Fig. S4j), indicative of a carboxyl group. Considering the
364 degree of unsaturation of the $C_8H_5NO_2$ molecule and the cyano group feature in BB tracers (e.g.,
365 hydrogen cyanide, benzonitrile) (Schneider et al., 1997; Li et al., 2000; Gilman et al., 2015),
366 $C_8H_5NO_2$ may be a cyanobenzoic acid.

367 The $C_{10}H_{11}NO_4$, $C_{10}H_{11}NO_5$, $C_{11}H_{13}NO_5$, and $C_{11}H_{13}NO_6$ detected here are also observed
368 in other BB experiments (Xie et al., 2019). Their MS-MS spectra are characterized by the loss of
369 at least one CH_3 and/or OCN (Fig. S4r–u), suggestive of methoxy or cyanate groups. Without



370 authentic standards, fragmentation patterns (Fig. S4r–u) were used to determine the molecular
371 structures of $C_{10}H_{11}NO_4$, $C_{10}H_{11}NO_5$, $C_{11}H_{13}NO_5$, and $C_{11}H_{13}NO_6$ (Table S3).

372 Nearly all NAC formulas identified in this work were observed previously (Lin et al., 2016,
373 2017; Xie et al., 2017a; Fleming et al., 2018; Xie et al., 2019). Few studies attempt to retrieve
374 structural information for NACs using MS-MS spectra of authentic standards. Although multiple
375 NACs may be generated from BB and photooxidation of aromatics in the presence of NO_x , NAC
376 structures may differ across emission sources. Xie et al. (2019) found that fragmentation patterns
377 of $C_7H_7NO_5$ and $C_8H_9NO_5$ from BB and photochemical reactions are distinct, and the methoxy
378 and cyanate groups are featured only in BB NACs. Thus, knowing the NAC structure is useful to
379 emissions source identification. In this work, the chemical and structural information obtained for
380 NACs sampled during red oak and charcoal burning are similar, presumably because the charcoal
381 fuel used is produced by the slow pyrolysis of wood. However, NACs in red oak and charcoal
382 burning emissions can be differentiated compositionally. As shown in Figs. 1 and S2, the NAC
383 emissions from red oak burning in cookstoves are characterized by $C_{10}H_7NO_3$ and $C_{11}H_9NO_3$. In
384 addition to these two species, charcoal burning in cookstoves also generates high fractions of
385 $C_8H_9NO_5$ (Fig. S2c, d). This difference among NACs may help with source apportionment. Figure
386 2 compares NAC composition from cookstove emissions, open BB (Xie et al., 2019), and SOA
387 chamber experiments (Xie et al., 2017a). Since previous source emissions studies ignored Q_b
388 measurements and normalized individual NACs concentrations to OM, only Q_f measurements in
389 this work are compared (Fig. 2a, b) with their $iNAC_{OC}\%$ values multiplied by 1.7 (proposed
390 OM/OC ratio, Reff et al., 2009). The three open BB tests (Fig. 2c) were conducted with two fuel
391 types under different ambient temperatures (10–29 °C) and RH% (49–83%) (Xie et al., 2019). But
392 they consistently emit $C_6H_5NO_4$, $C_7H_7NO_4$, and $C_9H_9NO_4$, which is compositionally distinct from



393 cookstove emissions (Fig. 2a, b). Moreover, the average mass contribution of total NACs to OM
394 for open BB ($0.12 \pm 0.051\%$) was 4–14 times lower than that for cookstove emissions. This result
395 is likely due to the high temperature flaming combustion produced in the cookstoves (Shen et al.,
396 2012; Xie et al., 2018). In Fig. 2d and e, the NAC profiles yielded for photochemical reactions
397 appear to have aromatic precursors. Therefore, the source of NACs can be identified by combining
398 their characteristic structures and composition. The filter-based NACs reported for the experiments
399 shown in Figure 2 were all measured using the identical method and HPLC-Q-ToFMS instrument,
400 reducing any potential methodological bias. However, total gas-phase NAC concentrations need
401 to be properly sampled and measured to account for the impact of gas/particle partitioning on their
402 distribution.

403 **3.4 Contributions of NACs to Abs_{365}**

404 The average $Abs_{365,iNAC\%}$ values of Q_f and Q_b samples are presented by fuel type and WBT
405 phase in the Fig. 3 stack plots, and experimental data for each fuel-cookstove are provided in
406 Tables S9–S12. The average contributions of total NACs to Abs_{365} ($Abs_{365,iNAC\%}$) of the sample
407 extracts (Q_f 1.10 – 2.58%, Q_b 10.7 – 21.0%) are up to 10 times greater than their average $tNAC_{OC\%}$
408 (Q_f 0.31 – 0.97%, Q_b 1.08 – 3.31%, Table 1). Considering that some NACs are not light-absorbing
409 (Table S4) and the OM/OC ratio is typically greater than unity, most NACs that contribute to
410 Abs_{365} are strong BrC chromophores. Like the mass composition of NACs (Fig. 1), $C_{10}H_7NO_3$ (CS
411 0.24%, HS 0.43%) and $C_8H_9NO_5$ (CS 1.22%, HS 0.55%) were the major contributors to Abs_{365}
412 for the Q_f samples collected during red oak and charcoal burning, respectively (Fig.3a). However,
413 the identified NACs only explain a minor fraction (< 5%) of bulk extract absorption. Chen and
414 Bond (2010) hypothesized that BrC absorption is strongly associated with large molecules
415 containing conjugated aromatic rings and functional groups. Additionally, Di Lorenzo et al. (2017)



416 demonstrated that the majority of BrC absorption arises from large molecules with MW > 500–
417 1000 Da. In previous studies, less than 10% of the BrC absorption at $\lambda = 365$ nm from ambient or
418 BB particles are ascribed to NACs with MW < 300 Da. Further studies are needed to identify these
419 larger molecules that are the dominant light absorbers in BB and cookstove PM. The average
420 $Abs_{365,tNAC\%}$ of Q_b samples are 7.52 to 11.3 times higher than those of Q_f samples. Unlike the Q_f
421 samples from red oak burning, $C_{10}H_{11}NO_5$ (CS 2.77%, HS 3.09%) has the highest average
422 contribution to Abs_{365} for Q_b samples, followed by $C_{10}H_7NO_3$ (CS 1.96%, HS 1.32%) and
423 $C_8H_9NO_5$ (CS 1.32%, HS 1.44%). While $C_8H_9NO_5$ dominated the contribution (CS 8.78%, HS
424 5.82%) to Abs_{365} for the Q_b samples from charcoal burning (Fig. 3b). As mentioned in section 3.2,
425 some NACs identified in this work might have substantial gas-phase concentrations. Jacobson
426 (1999) inferred that the nitrate-bearing aromatic gases may play a role in reducing the UV
427 irradiance within the boundary layer in Los Angeles during 1973 – 1987. Therefore, we suspect that
428 gaseous NACs may be an important group of molecules absorbing in short UV region in the
429 atmosphere.

430 **4 Conclusion**

431 This study investigated the composition, chemical formulas, and structures of NACs in
432 $PM_{2.5}$ emitted from burning red oak and charcoal in a variety of cookstoves. Total NAC mass and
433 compositional differences between Q_f and Q_b samples suggest that the identified NACs have
434 substantial gas-phase concentrations. By comparing the MS-MS spectra of identified NACs to
435 standard compound spectra, the structures of NACs featuring methoxy and cyanate groups in
436 cookstove emissions are confirmed. The source identification of NACs would be less ambiguous
437 if both the structures and composition of NACs are known, as different emission sources have
438 distinct NAC characteristics. Similar to previous work, the average contribution of total NACs to



439 Abs₃₆₅ of Q_f samples is less than 5% (1.10 – 2.58%), suggesting the need to shift our focus from
440 NACs (MW < 300 Da) to the chemical and optical properties of large molecules (e.g., MW > 500
441 Da) in particles. However, their average contributions to Abs₃₆₅ of Q_b samples are 7.52 to 11.3
442 times higher, so NACs may be important light absorbers in the gas phase. Further research in
443 understanding the influence of gaseous chromophores on the earth's radiative balance is warranted.

444

445 *Data availability*

446 Data used in the writing of this manuscript is available at the U.S. Environmental Protection
447 Agency's Environmental Dataset Gateway (<https://edg.epa.gov>).

448

449 *Competing interests*

450 The authors declare that they have no conflict of interest.

451

452 *Disclaimer*

453 The views expressed in this article are those of the authors and do not necessarily represent the
454 views or policies of the U.S. Environmental Protection Agency.

455

456 *Author contribution*

457 MX and AH designed the research. MX, ZZ, and XC performed the experiments. GS and JJ
458 managed sample collection. MX and MH analyzed the data and wrote the paper with significant
459 contributions from AH and QW.

460

461 *Acknowledgements*



462 This research was supported by the National Natural Science Foundation of China (NSFC,
463 41701551), the Startup Foundation for Introducing Talent of NUIST (No. 2243141801001), and
464 in part by an appointment to the Postdoctoral Research Program at the Office of Research and
465 Development by the Oak Ridge institute for Science and Education through Interagency
466 Agreement No. 92433001 between the U.S. Department of Energy and the U.S. Environmental
467 Protection Agency. We thank B. Patel for assistance on ECOC analysis of PM_{2.5} filters.

468

469 References

- 470 Anenberg, S. C., Balakrishnan, K., Jetter, J., Masera, O., Mehta, S., Moss, J., and Ramanathan, V.: Cleaner cooking
471 solutions to achieve health, climate, and economic cobenefits, *Environmental Science & Technology*, 47, 3944-
472 3952, 10.1021/es304942e, 2013.
- 473 Aunan, K., Berntsen, T. K., Myhre, G., Rypdal, K., Streets, D. G., Woo, J.-H., and Smith, K. R.: Radiative forcing
474 from household fuel burning in Asia, *Atmospheric Environment*, 43, 5674-5681,
475 <https://doi.org/10.1016/j.atmosenv.2009.07.053>, 2009.
- 476 Bond, T. C., Streets, D. G., Yarber, K. F., Nelson, S. M., Woo, J.-H., and Klimont, Z.: A technology-based global
477 inventory of black and organic carbon emissions from combustion, *Journal of Geophysical Research:*
478 *Atmospheres*, 109, 10.1029/2003jd003697, 2004.
- 479 Bonjour, S., Adair-Rohani, H., Wolf, J., Bruce Nigel, G., Mehta, S., Prüss-Ustün, A., Lahiff, M., Rehfuess Eva, A.,
480 Mishra, V., and Smith Kirk, R.: Solid fuel use for household cooking: Country and regional estimates for 1980-
481 2010, *Environmental Health Perspectives*, 121, 784-790, 10.1289/ehp.1205987, 2013.
- 482 Cao, G., Zhang, X., and Zheng, F.: Inventory of black carbon and organic carbon emissions from China, *Atmospheric*
483 *Environment*, 40, 6516-6527, <https://doi.org/10.1016/j.atmosenv.2006.05.070>, 2006.
- 484 Chen, Y., Sheng, G., Bi, X., Feng, Y., Mai, B., and Fu, J.: Emission Factors for carbonaceous particles and polycyclic
485 aromatic hydrocarbons from residential coal combustion in China, *Environmental Science & Technology*, 39,
486 1861-1867, 10.1021/es0493650, 2005.
- 487 Chen, Y., and Bond, T. C.: Light absorption by organic carbon from wood combustion, *Atmospheric Chemistry and*
488 *Physics*, 10, 1773-1787, 10.5194/acp-10-1773-2010, 2010.
- 489 Claeys, M., Vermeylen, R., Yasmeen, F., Gómez-González, Y., Chi, X., Maenhaut, W., Mészáros, T., and Salma, I.:
490 Chemical characterisation of humic-like substances from urban, rural and tropical biomass burning environments
491 using liquid chromatography with UV/vis photodiode array detection and electrospray ionisation mass
492 spectrometry, *Environmental Chemistry*, 9, 273-284, <https://doi.org/10.1071/EN11163>, 2012.
- 493 De Haan, D. O., Hawkins, L. N., Welsh, H. G., Pednekar, R., Casar, J. R., Pennington, E. A., de Loera, A., Jimenez,
494 N. G., Symons, M. A., Zauscher, M., Pajunoja, A., Caponi, L., Cazaunau, M., Formenti, P., Gratien, A., Pangui,
495 E., and Doussin, J.-F.: Brown carbon production in ammonium- or amine-containing aerosol particles by reactive
496 uptake of methylglyoxal and photolytic cloud cycling, *Environmental Science & Technology*, 51, 7458-7466,
497 10.1021/acs.est.7b00159, 2017.
- 498 Desyaterik, Y., Sun, Y., Shen, X., Lee, T., Wang, X., Wang, T., and Collett, J. L.: Speciation of “brown” carbon in
499 cloud water impacted by agricultural biomass burning in eastern China, *Journal of Geophysical Research:*
500 *Atmospheres*, 118, 7389-7399, 10.1002/jgrd.50561, 2013.
- 501 Di Lorenzo, R. A., Washenfelder, R. A., Attwood, A. R., Guo, H., Xu, L., Ng, N. L., Weber, R. J., Baumann, K.,
502 Edgerton, E., and Young, C. J.: Molecular-size-separated brown carbon absorption for biomass-burning aerosol
503 at multiple field sites, *Environmental Science & Technology*, 51, 3128-3137, 10.1021/acs.est.6b06160, 2017.
- 504 Donahue, N. M., Epstein, S. A., Pandis, S. N., and Robinson, A. L.: A two-dimensional volatility basis set: I.
505 organic-aerosol mixing thermodynamics, *Atmospheric Chemistry and Physics*, 11, 3303-3318, 10.5194/acp-11-
506 3303-2011, 2011.



- 507 Feng, Y., Ramanathan, V., and Kotamarthi, V. R.: Brown carbon: a significant atmospheric absorber of solar
508 radiation?, *Atmospheric Chemistry and Physics*, 13, 8607-8621, 10.5194/acp-13-8607-2013, 2013.
- 509 Fleming, L. T., Lin, P., Laskin, A., Laskin, J., Weltman, R., Edwards, R. D., Arora, N. K., Yadav, A., Meinardi, S.,
510 Blake, D. R., Pillarisetti, A., Smith, K. R., and Nizkorodov, S. A.: Molecular composition of particulate matter
511 emissions from dung and brushwood burning household cookstoves in Haryana, India, *Atmospheric Chemistry
512 and Physics*, 18, 2461-2480, 10.5194/acp-18-2461-2018, 2018.
- 513 Forrister, H., Liu, J., Scheuer, E., Dibb, J., Ziemba, L., Thornhill, K. L., Anderson, B., Diskin, G., Perring, A. E.,
514 Schwarz, J. P., Campuzano-Jost, P., Day, D. A., Palm, B. B., Jimenez, J. L., Nenes, A., and Weber, R. J.: Evolution
515 of brown carbon in wildfire plumes, *Geophysical Research Letters*, 42, 4623-4630, 10.1002/2015gl063897, 2015.
- 516 Gilman, J. B., Lerner, B. M., Kuster, W. C., Goldan, P. D., Warneke, C., Veres, P. R., Roberts, J. M., de Gouw, J. A.,
517 Burling, I. R., and Yokelson, R. J.: Biomass burning emissions and potential air quality impacts of volatile organic
518 compounds and other trace gases from fuels common in the US, *Atmospheric Chemistry and Physics*, 15, 13915-
519 13938, 10.5194/acp-15-13915-2015, 2015.
- 520 Glarborg, P., Jensen, A., and Johnsson, J. E.: Fuel nitrogen conversion in solid fuel fired systems, *Progress in Energy
521 and Combustion Science*, 29, 89-113, 2003.
- 522 Global Alliance for Clean Cookstoves, 2014. Water Boiling Test (WBT) 4.2.3. Released 19 March 2014
523 <http://cleancookstoves.org/technology-and-fuels/testing/protocols.html> (accessed July 2017).
- 524 Harrison, M. A., Barra, S., Borghesi, D., Vione, D., Arsene, C., and Olariu, R. I.: Nitrated phenols in the atmosphere:
525 a review, *Atmospheric Environment*, 39, 231-248, 2005.
- 526 Hecobian, A., Zhang, X., Zheng, M., Frank, N., Edgerton, E. S., and Weber, R. J.: Water-Soluble Organic Aerosol
527 material and the light-absorption characteristics of aqueous extracts measured over the Southeastern United States,
528 *Atmospheric Chemistry and Physics*, 10, 5965-5977, 10.5194/acp-10-5965-2010, 2010.
- 529 Iinuma, Y., Böge, O., Gräfe, R., and Herrmann, H.: Methyl-nitrocatechols: Atmospheric tracer compounds for
530 biomass burning secondary organic aerosols, *Environmental Science & Technology*, 44, 8453-8459,
531 10.1021/es102938a, 2010.
- 532 International Agency for Research on Cancer (IARC): Some non-heterocyclic polycyclic aromatic hydrocarbons and
533 some related exposures (Vol. 92). IARC Press, International Agency for Research on Cancer, 2010.
- 534 Jacobson, M. Z.: Isolating nitrated and aromatic aerosols and nitrated aromatic gases as sources of ultraviolet light
535 absorption, *Journal of Geophysical Research: Atmospheres*, 104, 3527-3542, 10.1029/1998jd100054, 1999.
- 536 Jaeckels, J. M., Bae, M. S., and Schauer, J. J.: Positive matrix factorization (PMF) analysis of molecular marker
537 measurements to quantify the sources of organic aerosols, *Environmental Science & Technology*, 41, 5763-5769,
538 10.1021/es062536b, 2007.
- 539 Jetter, J., Zhao, Y., Smith, K. R., Khan, B., Yelverton, T., DeCarlo, P., and Hays, M. D.: Pollutant emissions and
540 energy efficiency under controlled conditions for household biomass cookstoves and implications for metrics
541 useful in setting international test standards, *Environmental Science & Technology*, 46, 10827-10834,
542 10.1021/es301693f, 2012.
- 543 Kaal, J., Martínez Cortizas, A., and Nierop, K. G. J.: Characterisation of aged charcoal using a coil probe pyrolysis-
544 GC/MS method optimised for black carbon, *Journal of Analytical and Applied Pyrolysis*, 85, 408-416,
545 <https://doi.org/10.1016/j.jaap.2008.11.007>, 2009.
- 546 Kim, K.-H., Jahan, S. A., Kabir, E., and Brown, R. J. C.: A review of airborne polycyclic aromatic hydrocarbons
547 (PAHs) and their human health effects, *Environment International*, 60, 71-80,
548 <https://doi.org/10.1016/j.envint.2013.07.019>, 2013.
- 549 Kim Oanh, N. T., Betz Reutergårdh, L., and Dung, N. T.: Emission of polycyclic aromatic hydrocarbons and
550 particulate matter from domestic combustion of selected fuels, *Environmental Science & Technology*, 33, 2703-
551 2709, 10.1021/es980853f, 1999.
- 552 Klimont, Z., Cofala, J., Xing, J., Wei, W., Zhang, C., Wang, S., Kejun, J., Bhandari, P., Mathur, R., Purohit, P., Rafaj,
553 P., Chambers, A., Amann, M., and Hao, J.: Projections of SO₂, NO_x and carbonaceous aerosols emissions in
554 Asia, *Tellus B*, 61, 602-617, 10.1111/j.1600-0889.2009.00428.x, 2009.
- 555 Kwamena, N.-O., and Abbatt, J.: Heterogeneous nitration reactions of polycyclic aromatic hydrocarbons and n-hexane
556 soot by exposure to NO₃/NO₂/N₂O₅, *Atmospheric Environment*, 42, 8309-8314, 2008.
- 557 Lacey, F., and Henze, D.: Global climate impacts of country-level primary carbonaceous aerosol from solid-fuel
558 cookstove emissions, *Environmental Research Letters*, 10, 114003, 10.1088/1748-9326/10/11/114003, 2015.
- 559 Lei, Y., Zhang, Q., He, K. B., and Streets, D. G.: Primary anthropogenic aerosol emission trends for China, 1990-
560 2005, *Atmos. Chem. Phys.*, 11, 931-954, 10.5194/acp-11-931-2011, 2011.



- 561 Li, M., Wang, X., Lu, C., Li, R., Zhang, J., Dong, S., Yang, L., Xue, L., Chen, J., and Wang, W.: Nitrated phenols
562 and the phenolic precursors in the atmosphere in urban Jinan, China, *Science of The Total Environment*, 136760,
563 <https://doi.org/10.1016/j.scitotenv.2020.136760>, 2020.
- 564 Li, Q., Jacob, D. J., Bey, I., Yantosca, R. M., Zhao, Y., Kondo, Y., and Notholt, J.: Atmospheric hydrogen cyanide
565 (HCN): Biomass burning source, ocean sink?, *Geophysical Research Letters*, 27, 357-360,
566 [10.1029/1999gl1010935](https://doi.org/10.1029/1999gl1010935), 2000.
- 567 Lin, P., Aiona, P. K., Li, Y., Shiraiwa, M., Laskin, J., Nizkorodov, S. A., and Laskin, A.: Molecular characterization
568 of brown carbon in biomass burning aerosol particles, *Environmental Science & Technology*, 50, 11815-11824,
569 [10.1021/acs.est.6b03024](https://doi.org/10.1021/acs.est.6b03024), 2016.
- 570 Lin, P., Bluvshstein, N., Rudich, Y., Nizkorodov, S. A., Laskin, J., and Laskin, A.: Molecular chemistry of atmospheric
571 brown carbon inferred from a nationwide biomass burning event, *Environmental Science & Technology*, 51,
572 [11561-11570](https://doi.org/10.1021/acs.est.7b02276), [10.1021/acs.est.7b02276](https://doi.org/10.1021/acs.est.7b02276), 2017.
- 573 Lin, P., Liu, J. M., Shilling, J. E., Kathmann, S. M., Laskin, J., and Laskin, A.: Molecular characterization of brown
574 carbon (BrC) chromophores in secondary organic aerosol generated from photo-oxidation of toluene, *Physical
575 Chemistry Chemical Physics*, 17, 23312-23325, [10.1039/c5cp02563j](https://doi.org/10.1039/c5cp02563j), 2015.
- 576 Liu, J., Bergin, M., Guo, H., King, L., Kotra, N., Edgerton, E., and Weber, R. J.: Size-resolved measurements of brown
577 carbon in water and methanol extracts and estimates of their contribution to ambient fine-particle light absorption,
578 *Atmospheric Chemistry and Physics*, 13, 12389-12404, [10.5194/acp-13-12389-2013](https://doi.org/10.5194/acp-13-12389-2013), 2013.
- 579 Lu, C., Wang, X., Li, R., Gu, R., Zhang, Y., Li, W., Gao, R., Chen, B., Xue, L., and Wang, W.: Emissions of fine
580 particulate nitrated phenols from residential coal combustion in China, *Atmospheric Environment*, 203, 10-17,
581 <https://doi.org/10.1016/j.atmosenv.2019.01.047>, 2019.
- 582 Lu, J. W., Flores, J. M., Lavi, A., Abo-Riziq, A., and Rudich, Y.: Changes in the optical properties of benzo[a]pyrene-
583 coated aerosols upon heterogeneous reactions with NO₂ and NO₃, *Physical Chemistry Chemical Physics*, 13,
584 [6484-6492](https://doi.org/10.1039/C0CP02114H), [10.1039/C0CP02114H](https://doi.org/10.1039/C0CP02114H), 2011.
- 585 Lu, Z., Streets, D. G., Winijkul, E., Yan, F., Chen, Y., Bond, T. C., Feng, Y., Dubey, M. K., Liu, S., Pinto, J. P., and
586 Carmichael, G. R.: Light absorption properties and radiative effects of primary organic aerosol emissions,
587 *Environmental Science & Technology*, 49, 4868-4877, [10.1021/acs.est.5b00211](https://doi.org/10.1021/acs.est.5b00211), 2015.
- 588 McMeeking, G., Fortner, E., Onasch, T., Taylor, J., Flynn, M., Coe, H., and Kreidenweis, S.: Impacts of nonrefractory
589 material on light absorption by aerosols emitted from biomass burning, *Journal of Geophysical Research:
590 Atmospheres*, 119, 212,272-212,286, 2014.
- 591 Nakayama, T., Matsumi, Y., Sato, K., Imamura, T., Yamazaki, A., and Uchiyama, A.: Laboratory studies on optical
592 properties of secondary organic aerosols generated during the photooxidation of toluene and the ozonolysis of α-
593 pinene, *Journal of Geophysical Research: Atmospheres*, 115, n/a-n/a, [10.1029/2010jd014387](https://doi.org/10.1029/2010jd014387), 2010.
- 594 Park, R. J., Kim, M. J., Jeong, J. I., Youn, D., and Kim, S.: A contribution of brown carbon aerosol to the aerosol
595 light absorption and its radiative forcing in East Asia, *Atmospheric Environment*, 44, 1414-1421,
596 <https://doi.org/10.1016/j.atmosenv.2010.01.042>, 2010.
- 597 Peters, A. J., Lane, D. A., Gundel, L. A., Northcott, G. L., and Jones, K. C.: A comparison of high volume and diffusion
598 denuder samplers for measuring semivolatile organic compounds in the atmosphere, *Environmental Science &
599 Technology*, 34, 5001-5006, [10.1021/es000056t](https://doi.org/10.1021/es000056t), 2000.
- 600 Pokhrel, R. P., Wagner, N. L., Langridge, J. M., Lack, D. A., Jayarathne, T., Stone, E. A., Stockwell, C. E., Yokelson,
601 R. J., and Murphy, S. M.: Parameterization of single-scattering albedo (SSA) and absorption Ångström exponent
602 (AAE) with EC/OC for aerosol emissions from biomass burning, *Atmospheric Chemistry and Physics*, 16, 9549-
603 [9561](https://doi.org/10.5194/acp-16-9549-2016), [10.5194/acp-16-9549-2016](https://doi.org/10.5194/acp-16-9549-2016), 2016.
- 604 Ravindra, K., Sokhi, R., and Van Grieken, R.: Atmospheric polycyclic aromatic hydrocarbons: Source attribution,
605 emission factors and regulation, *Atmospheric Environment*, 42, 2895-2921,
606 <https://doi.org/10.1016/j.atmosenv.2007.12.010>, 2008.
- 607 Reff, A., Bhave, P. V., Simon, H., Pace, T. G., Pouliot, G. A., Mobley, J. D., and Houyoux, M.: Emissions inventory
608 of PM_{2.5} trace elements across the United States, *Environmental Science & Technology*, 43, 5790-5796,
609 [10.1021/es802930x](https://doi.org/10.1021/es802930x), 2009.
- 610 Riddle, S. G., Jakober, C. A., Robert, M. A., Cahill, T. M., Charles, M. J., and Kleeman, M. J.: Large PAHs detected
611 in fine particulate matter emitted from light-duty gasoline vehicles, *Atmospheric Environment*, 41, 8658-8668,
612 <https://doi.org/10.1016/j.atmosenv.2007.07.023>, 2007.
- 613 Saleh, R., Robinson, E. S., Tkacik, D. S., Ahern, A. T., Liu, S., Aiken, A. C., Sullivan, R. C., Presto, A. A., Dubey,
614 M. K., Yokelson, R. J., Donahue, N. M., and Robinson, A. L.: Brownness of organics in aerosols from biomass
615 burning linked to their black carbon content, *Nature Geoscience*, 7, 647-650, [10.1038/ngeo2220](https://doi.org/10.1038/ngeo2220), 2014.



- 616 Samburova, V., Connolly, J., Gyawali, M., Yatavelli, R. L. N., Watts, A. C., Chakrabarty, R. K., Zielinska, B.,
617 Moosmüller, H., and Khlystov, A.: Polycyclic aromatic hydrocarbons in biomass-burning emissions and their
618 contribution to light absorption and aerosol toxicity, *Science of The Total Environment*, 568, 391-401,
619 <http://doi.org/10.1016/j.scitotenv.2016.06.026>, 2016.
- 620 Schneider, J., Bürger, V., and Arnold, F.: Methyl cyanide and hydrogen cyanide measurements in the lower
621 stratosphere: Implications for methyl cyanide sources and sinks, *Journal of Geophysical Research: Atmospheres*,
622 102, 25501-25506, 10.1029/97jd02364, 1997.
- 623 Shen, G., Tao, S., Wei, S., Zhang, Y., Wang, R., Wang, B., Li, W., Shen, H., Huang, Y., Chen, Y., Chen, H., Yang,
624 Y., Wang, W., Wei, W., Wang, X., Liu, W., Wang, X., and Simonich, S. L. M.: Reductions in Emissions of
625 Carbonaceous particulate matter and polycyclic aromatic hydrocarbons from combustion of biomass pellets in
626 comparison with raw fuel burning, *Environmental Science & Technology*, 46, 6409-6416, 10.1021/es300369d,
627 2012.
- 628 Shrivastava, M. K., Subramanian, R., Rogge, W. F., and Robinson, A. L.: Sources of organic aerosol: Positive matrix
629 factorization of molecular marker data and comparison of results from different source apportionment models,
630 *Atmospheric Environment*, 41, 9353-9369, 10.1016/j.atmosenv.2007.09.016, 2007.
- 631 Simoneit, B. R., Rogge, W., Mazurek, M., Standley, L., Hildemann, L., and Cass, G.: Lignin pyrolysis products,
632 lignans, and resin acids as specific tracers of plant classes in emissions from biomass combustion, *Environmental
633 science & technology*, 27, 2533-2541, 1993.
- 634 Simoneit, B. R.: Biomass burning—a review of organic tracers for smoke from incomplete combustion, *Applied
635 Geochemistry*, 17, 129-162, 2002.
- 636 Smith, K. R., Bruce, N., Balakrishnan, K., Adair-Rohani, H., Balmes, J., Chafe, Z., Dherani, M., Hosgood, H. D.,
637 Mehta, S., Pope, D., and Rehfuess, E.: Millions dead: How do we know and what does it mean? Methods used in
638 the comparative risk assessment of household air pollution, *Annual Review of Public Health*, 35, 185-206,
639 10.1146/annurev-publhealth-032013-182356, 2014.
- 640 Subramanian, R., Khlystov, A. Y., Cabada, J. C., and Robinson, A. L.: Positive and negative artifacts in particulate
641 organic carbon measurements with denuded and undenuded sampler configurations special issue of *Aerosol
642 Science and Technology* on findings from the fine particulate matter supersites program, *Aerosol Science and
643 Technology*, 38, 27-48, 10.1080/02786820390229354, 2004.
- 644 Sun, J., Zhi, G., Hitznerberger, R., Chen, Y., Tian, C., Zhang, Y., Feng, Y., Cheng, M., Cai, J., Chen, F., Qiu, Y., Jiang,
645 Z., Li, J., Zhang, G., and Mo, Y.: Emission factors and light absorption properties of brown carbon from household
646 coal combustion in China, *Atmospheric Chemistry and Physics*, 17, 4769-4780, 10.5194/acp-17-4769-2017, 2017.
- 647 Teich, M., van Pinxteren, D., Wang, M., Kecorius, S., Wang, Z., Müller, T., Močnik, G., and Herrmann, H.:
648 Contributions of nitrated aromatic compounds to the light absorption of water-soluble and particulate brown
649 carbon in different atmospheric environments in Germany and China, *Atmospheric Chemistry and Physics*, 17,
650 1653-1672, 10.5194/acp-17-1653-2017, 2017.
- 651 Tuccella, P., Curci, G., Pitari, G., Lee, S., and Jo, D. S.: Direct radiative effect of absorbing aerosols: sensitivity to
652 mixing state, brown carbon and soil dust refractive index and shape, *Journal of Geophysical Research:
653 Atmospheres*, 125, e2019JD030967, 10.1029/2019JD030967, 2020.
- 654 Turpin, B. J., and Lim, H.-J.: Species contributions to PM_{2.5} mass concentrations: Revisiting common assumptions
655 for estimating organic mass, *erosol Science and Technology*, 35, 602-610, 10.1080/02786820119445, 2001.
- 656 Wang, X., Heald, C. L., Ridley, D. A., Schwarz, J. P., Spackman, J. R., Perring, A. E., Coe, H., Liu, D., and Clarke,
657 A. D.: Exploiting simultaneous observational constraints on mass and absorption to estimate the global direct
658 radiative forcing of black carbon and brown carbon, *Atmospheric Chemistry and Physics*, 14, 10989-11010,
659 10.5194/acp-14-10989-2014, 2014.
- 660 Wathore, R., Mortimer, K., and Grieshop, A. P.: In-use emissions and estimated impacts of traditional, natural- and
661 forced-draft cookstoves in rural Malawi, *Environmental Science & Technology*, 51, 1929-1938,
662 10.1021/acs.est.6b05557, 2017.
- 663 Watson, J. G., Chow, J. C., Chen, L. W. A., and Frank, N. H.: Methods to assess carbonaceous aerosol sampling
664 artifacts for IMPROVE and other long-term networks, *Journal of the Air & Waste Management Association*, 59,
665 898-911, 10.3155/1047-3289.59.8.898, 2009.
- 666 Xie, M., Hannigan, M. P., Dutton, S. J., Milford, J. B., Hemann, J. G., Miller, S. L., Schauer, J. J., Peel, J. L., and
667 Vedal, S.: Positive matrix factorization of PM_{2.5}: Comparison and implications of using different speciation data
668 sets, *Environmental Science & Technology*, 46, 11962-11970, 10.1021/es302358g, 2012.
- 669 Xie, M., Hannigan, M. P., and Barsanti, K. C.: Gas/particle partitioning of n-alkanes, PAHs and oxygenated PAHs in
670 urban Denver, *Atmospheric Environment*, 95, 355-362, <http://dx.doi.org/10.1016/j.atmosenv.2014.06.056>, 2014.



- 671 Xie, M., Chen, X., Hays, M. D., Lewandowski, M., Offenberg, J., Kleindienst, T. E., and Holder, A. L.: Light
672 absorption of secondary organic aerosol: Composition and contribution of nitroaromatic compounds,
673 *Environmental Science & Technology*, 51, 11607-11616, 10.1021/acs.est.7b03263, 2017a.
- 674 Xie, M., Hays, M. D., and Holder, A. L.: Light-absorbing organic carbon from prescribed and laboratory biomass
675 burning and gasoline vehicle emissions, *Scientific Reports*, 7, 7318, 10.1038/s41598-017-06981-8, 2017b.
- 676 Xie, M., Shen, G., Holder, A. L., Hays, M. D., and Jetter, J. J.: Light absorption of organic carbon emitted from
677 burning wood, charcoal, and kerosene in household cookstoves, *Environmental Pollution*, 240, 60-67,
678 <https://doi.org/10.1016/j.envpol.2018.04.085>, 2018.
- 679 Xie, M., Chen, X., Hays, M. D., and Holder, A. L.: Composition and light absorption of N-containing aromatic
680 compounds in organic aerosols from laboratory biomass burning, *Atmospheric Chemistry and Physics*, 19, 2899-
681 2915, 10.5194/acp-19-2899-2019, 2019.
- 682 Yang, M., Howell, S. G., Zhuang, J., and Huebert, B. J.: Attribution of aerosol light absorption to black carbon,
683 brown carbon, and dust in China – interpretations of atmospheric measurements during EAST-AIRE,
684 *Atmospheric Chemistry and Physics*, 9, 2035-2050, 10.5194/acp-9-2035-2009, 2009.
- 685 Zhang, X., Lin, Y.-H., Surratt, J. D., and Weber, R. J.: Sources, composition and absorption Ångström exponent of
686 light-absorbing organic components in aerosol extracts from the Los Angeles basin, *Environmental Science &*
687 *Technology*, 47, 3685-3693, 10.1021/es305047b, 2013.



Table 1. Average concentrations of total NACs and tNAC_{OC}% in Q_f and Q_b samples by fuel type and WBT phase.

| Fuel & Test phase | Red Oak | | Charcoal | |
|--|-----------------|-----------------|-----------------|-------------------|
| | CS | HS ^a | CS | HS |
| Front filter (Q_f) | | | | |
| Sample number | 18 | 17 ^b | 15 | 15 |
| total NAC ($\mu\text{g m}^{-3}$) | 3.22 ± 1.36 | 3.54 ± 1.63 | 0.47 ± 0.40 | 0.97 ± 0.46 |
| tNAC _{OC} % | 0.97 ± 1.07 | 0.94 ± 1.10 | 0.38 ± 0.25 | 0.31 ± 0.22 |
| OC ($\mu\text{g m}^{-3}$) ^c | 624 ± 410 | 908 ± 885 | 115 ± 72.0 | 447 ± 271 |
| EC/OC ^c | 1.74 ± 1.42 | 1.96 ± 1.74 | 6.12 ± 2.76 | 0.029 ± 0.012 |
| Backup filter (Q_b) | | | | |
| Sample number | 18 | 17 ^b | 14 ^b | 15 |
| total NAC ($\mu\text{g m}^{-3}$) | 1.67 ± 0.76 | 1.78 ± 0.78 | 0.37 ± 0.31 | 1.30 ± 0.70 |
| tNAC _{OC} % | 3.31 ± 3.46 | 2.76 ± 2.67 | 1.10 ± 0.89 | 1.08 ± 0.51 |
| OC ($\mu\text{g m}^{-3}$) ^c | 78.4 ± 43.2 | 100 ± 58.4 | 41.9 ± 23.3 | 138 ± 70.8 |
| Q_b/Q_f ratio (%) | | | | |
| total NACs | 53.0 ± 10.6 | 55.1 ± 24.7 | 87.7 ± 34.2 | 143 ± 51.4 |
| OC ^c | 14.8 ± 3.87 | 15.3 ± 6.37 | 35.4 ± 12.2 | 38.8 ± 18.9 |

^a Including three SIM phase samples from the 3-stone fire; ^b one filter sample was missed for analysis; ^c data were obtained from Xie et al. (2018).

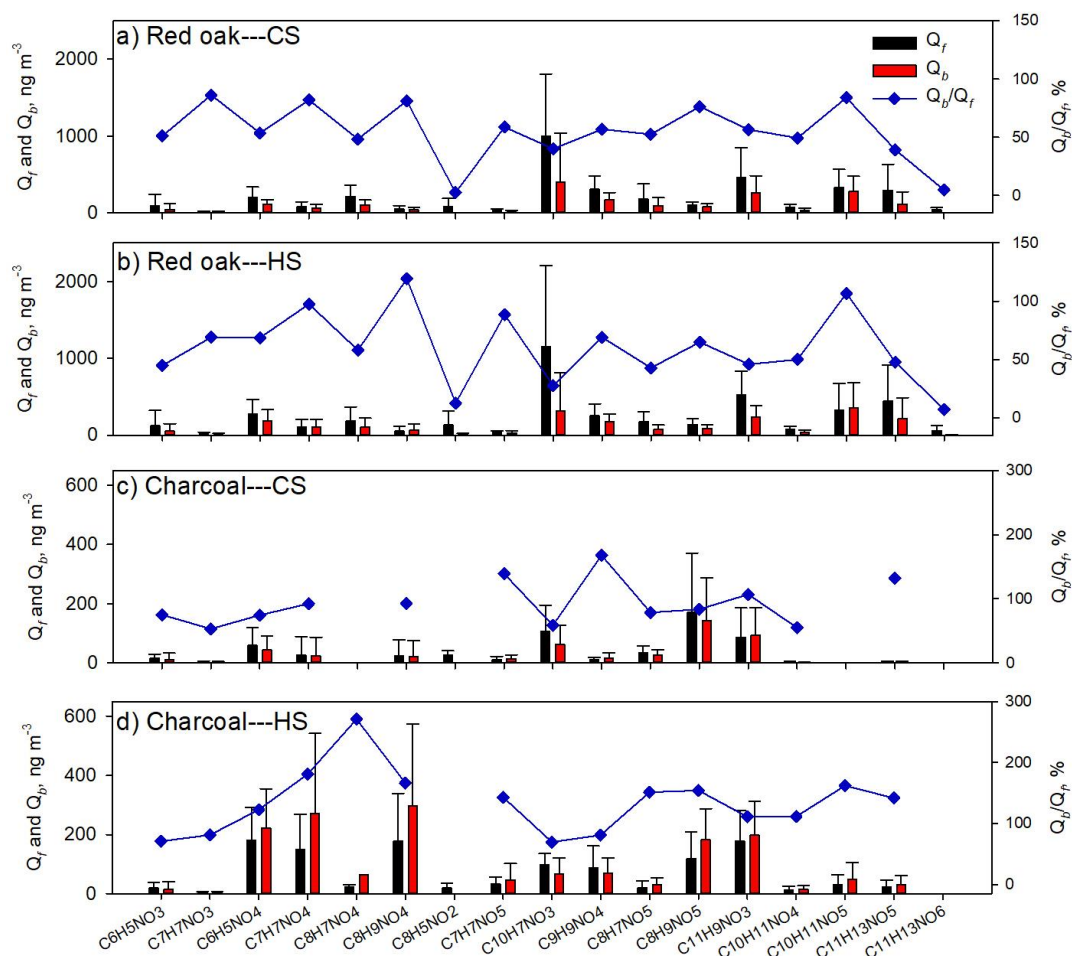


Figure 1. Average concentrations of individual NACs in Q_f and Q_b samples for (a) red oak burning under the CS phase, (b) red oak burning under the HS phase, (c) charcoal burning under the CS phase, and (d) charcoal burning under the HS phase. The blue scatters in each plot are mass ratios of individual NACs in Q_b to Q_f samples $\times 100\%$.

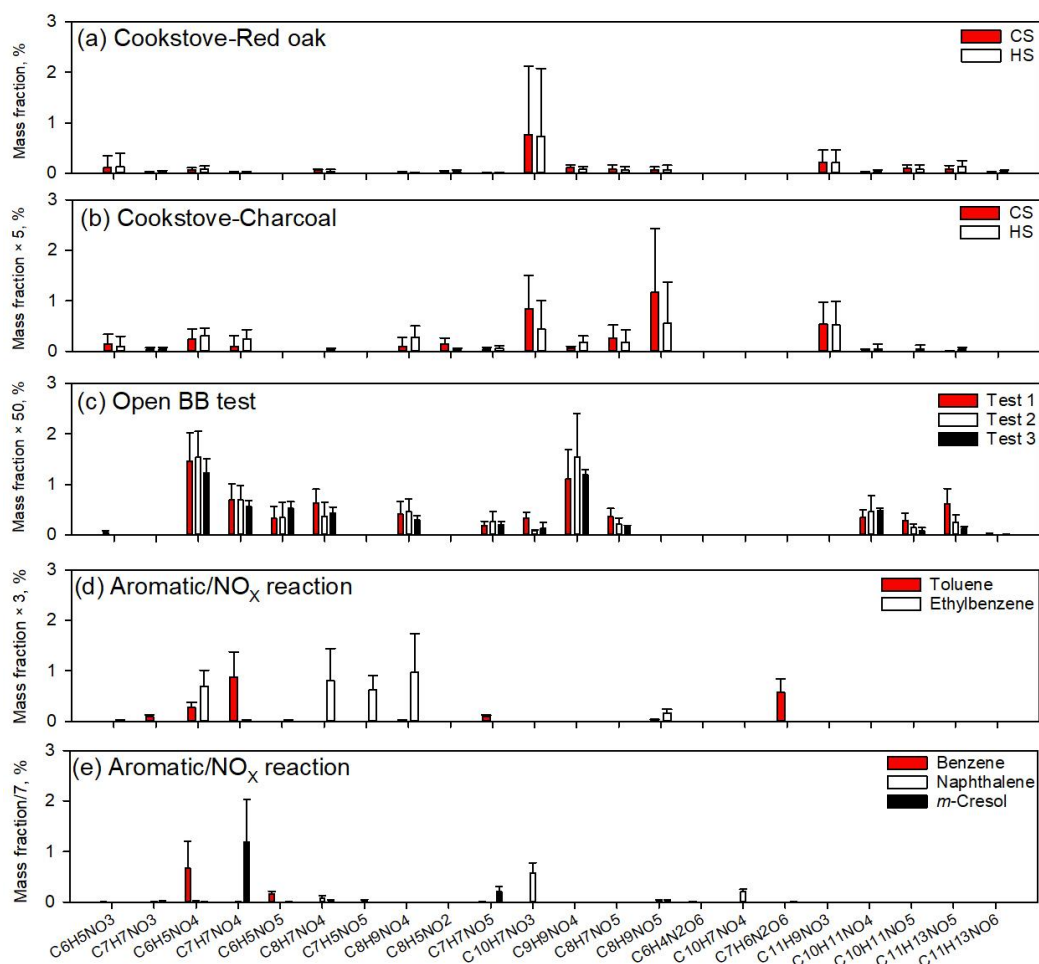


Figure 2. Average mass ratios (%) of individual NACs to organic matter from (a) red oak burning in cookstoves, (b) charcoal burning in cookstoves, (c) open BB experiments (Xie et al., 2019), photochemical reactions of (d) toluene and ethylbenzene, and (e) benzene, naphthalene, and *m*-cresol with NO_x (Xie et al., 2017a).

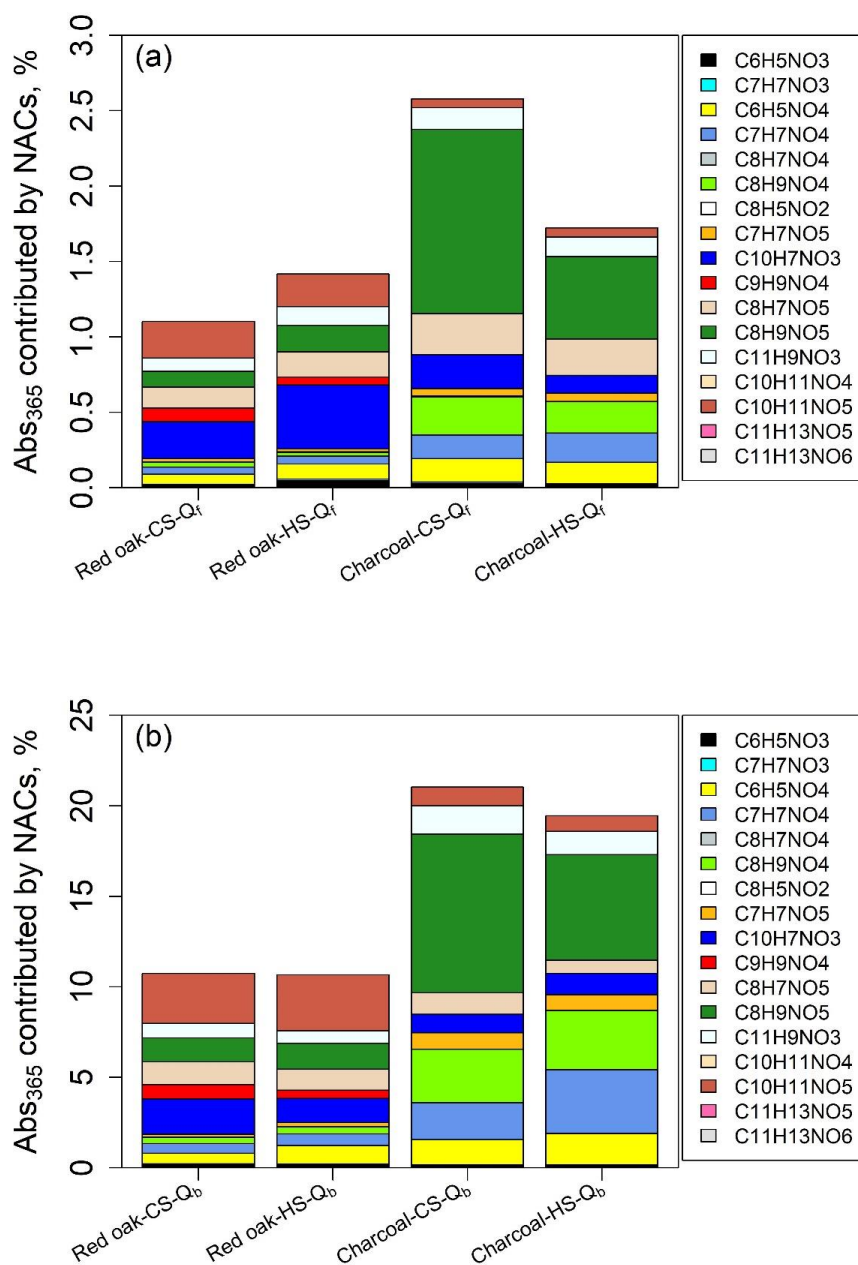


Figure 3. Average contributions (%) of individual NACs to bulk extracts Abs₃₆₅ of (a) Q_f, and (b) Q_b samples from burning red oak and charcoal in cookstoves under CS and HS phases.